

## Water-gas-shift kinetic over nano-structured iron catalyst in Fischer–Tropsch synthesis

Ali Nakhaei Pour<sup>a,b,\*</sup>, Mohammad Reza Housaindokht<sup>a</sup>, Jamshid Zarkesh<sup>b</sup>, Sayyed Faramarz Tayyari<sup>a</sup>

<sup>a</sup> Department of Chemistry, Ferdowsi university of Mashhad, P.O. Box: 91775-1436, Mashhad, Iran

<sup>b</sup> Research Institute of Petroleum Industry of National Iranian Oil Company; P.O. Box: 137-14665, Tehran, Iran

### ARTICLE INFO

#### Article history:

Received 25 February 2010

Received in revised form

10 April 2010

Accepted 15 April 2010

Available online 20 May 2010

#### Keywords:

Fischer–Tropsch synthesis

Water-gas-shift reaction

Iron catalyst

Kinetics

### ABSTRACT

Kinetic modeling of the water-gas-shift (WGS) reaction over a nano-structured iron catalyst under Fischer–Tropsch synthesis (FTS) reaction conditions is investigated. The Fe/Cu/La/Si nano-structured catalyst was prepared by co-precipitation in a water-in-oil microemulsion. A number of Langmuir–Hinshelwood–Hougen–Watson type rate equations based on possible reactions sets originated from the formate and direct oxidation mechanisms, are derived. By considering experimental data measured over a wide range of reaction conditions, discrimination between the various rate equations is investigated during this study. WGS rate expressions based on the formate mechanism were found to provide an improved description of the WGS kinetic data.

© 2010 Elsevier B.V. All rights reserved.

### 1. Introduction

The Fischer–Tropsch synthesis (FTS) has been recognized as an important alternate technology to petroleum refining in the production of liquid fuels and chemicals from syngas derived from coal, natural gas and other carbon-containing materials (Anderson, 1984; Bartholomew, 1991; Dry, 1981). Fe-based catalyst is often selected for the FTS, over its competitor of Co-based catalyst, because of its water-gas-shift (WGS) activity to working in a wide range of H<sub>2</sub>/CO feed ratio. The FTS and WGS reactions can be shown as:



where  $n$  is the average H/C ratio of the produced hydrocarbons. The WGS reaction is a reversible parallel-consecutive reaction with respect to CO and assumed that carbon dioxide is essentially formed by this reaction (Jothimurugesan et al., 2000; Jin and Datye, 2000; Nakhaei Pour et al., 2008a,b,c). It is generally accepted that the FTS and WGS reactions take place on different active sites on a precipitated iron catalyst and the two reactions will only influence each other via the gas phase of reactants. Literature suggests

that the formation of iron carbides result in a high FTS activity, and the magnetite (Fe<sub>3</sub>O<sub>4</sub>) is the most active phase for WGS reaction (Van der Laan and Beenackers, 1999, 2000; Wang et al., 2003; Guo et al., 2006; Teng et al., 2005). Thus the FTS (hydrocarbon formation) and WGS (carbon dioxide formation) reactions can be described with separate kinetic expressions.

Recent studies showed that nanosized iron particles were essential to achieve high FTS activity. Some authors prepared supported iron-based Fischer–Tropsch catalysts with microemulsion method, and reported high activity and selectivity to oxygenate (Nakhaei Pour et al., 2009a,b, 2010a,b; Sarkar et al., 2007; Herranz et al., 2006; Eriksson et al., 2004). A microemulsion is optically transparent and has thermodynamically stable dispersion of water phase into an organic phase that stabilized by a surfactant (Schwuger et al., 1995).

The objective of this work is to systemically establish and discriminate Langmuir–Hinshelwood–Hogen–Watson (LHHW) kinetics model for the WGS reaction on the basis of possible detailed mechanism over a nanostructure Fe/Cu/La/Si catalyst under FTS reaction conditions. By using the experimentally data, a set of WGS kinetic models are estimated and discriminated separately.

### 2. Experimental

#### 2.1. Catalyst preparation

The Fe/Cu/La/Si nano-catalyst precursors were prepared by co-precipitation in a water-in-oil microemulsion as described

\* Corresponding author. Department of Chemistry, Ferdowsi university of Mashhad, P.O. Box: 91775-1436, Mashhad, Iran. Tel./fax: +98 21 44739716.

E-mail addresses: [nakhaeipoura@ripi.ir](mailto:nakhaeipoura@ripi.ir), [nakhaeipoura@yahoo.com](mailto:nakhaeipoura@yahoo.com) (A. Nakhaei Pour).

previously (Nakhaei Pour et al., 2009a,b, 2010a,b). The promoted catalysts were dried at 383 K for 16 h and calcined at 773 K for 3 h in air. The catalyst compositions were designed in terms of the atomic ratios as: 100Fe/5.64Cu/2La/19Si. Based on previous results, the crystal size of the nano catalyst was determined 20 nm (Nakhaei Pour et al., 2009a,b, 2010a,b).

## 2.2. Catalytic performance

Steady-state FTS reaction rates and selectivities were measured in a continuous spinning basket reactor (stainless steel,  $H = 0.122$  m,  $D_0 = 0.052$  m,  $D_i = 0.046$  m) with temperature controllers (WEST series 3800). A J-type movable thermocouple made it possible to monitor the bed temperature axially, which was within 0.5 K of the average bed temperature. The reactor system also included a 50 cm<sup>3</sup> stainless steel cold trap at ambient temperature located before the gas chromatograph sampling valve. Incondensable gases were passed through sampling valve into an online gas chromatograph continuously then vent through a soap-film bubble meter. Separate Brooks 5850 mass flow controllers were used to add H<sub>2</sub> and CO at the desired rate in admixing vessel that was preceded by a palladium trap and a molecular sieve trap to remove metal carbonyls and water before entering to the reactor. A compact pressure controller was used to control the pressure. The flow rate of tail gas is measured by a wet test gas meter.

Blank experiments showed that the spinning basket reactor charged with inert silica sand without the catalyst has no conversion of syngas. The fresh catalyst is crushed and sieved to particles with the diameter of 0.25–0.36 mm (40–60 ASTM mesh). The weight of the catalyst loaded was 2.5 g and diluted by 30 cm<sup>3</sup> inert silica sand with the same mesh size range. The catalyst samples were activated by a 5% (v/v) H<sub>2</sub>/N<sub>2</sub> gas mixture with space velocity equal to 15.1 nl h<sup>-1</sup> g<sub>Fe</sub><sup>-1</sup> at 0.1 Mpa and 1800 rpm. The reactor temperature increased to 673 K with a heating rate of 5 K/min, maintained for 1 h at this temperature, and then reduced to 543 K. The activation is followed by the synthesis gas stream with H<sub>2</sub>/CO = 1 and space velocity of 3.07 nl h<sup>-1</sup> g<sub>Fe</sub><sup>-1</sup> for 24 h in 0.1 MPa and 543 K before setting the actual reaction temperature and pressure. After catalyst reduction, synthesis gas was feed to the reactor at conditions operated at 563 K, 1.7 MPa, (H<sub>2</sub>/CO) feed = 1 and a space velocity of 10.4 nl h<sup>-1</sup> g<sub>Fe</sub><sup>-1</sup>. A stabilization period of 15 h is conducted under the reaction conditions, and then the kinetic measurement was carried out. After the process conditions are changed, at least 12 h is used for the system stabilization before a new mass balance period. After reaching steady-state activity and selectivity, the kinetics of the WGS measured.

The external mass transfer limitation is investigated by comparing the CO conversions under different stirring speeds of the reactor. Apparently the stirring speed needed to eliminate the external mass transfer limitation that correspondingly increases with the increase of the reaction temperature. This is due to the fact that, the relative rate of external mass transfer versus the reaction rate decreases with the increasing of temperature. Therefore, the corresponding stirring speed should ensure that the experimental data measured are in the kinetically limited regime. In our experiments, all the experiments are carried out at 1800 rpm which is safe to eliminate the external mass transfer limitations for all kinetic conditions. Our extensive experimental results proved that the particle diameter used in this experiment is safe for negligible intra-particle diffusion limitations. The kinetic parameters optimization later in this paper also indicates that the experimental results are free from the external and internal mass transfer limitations and in the kinetically limited regime.

During the entire runs, the reactor temperature varied between 543 and 593 K, the pressure was 1.7 MPa, and the space velocity of the synthesis gas varied between 3.5 and 28.7 nl h<sup>-1</sup> g<sub>Fe</sub><sup>-1</sup>. The H<sub>2</sub>/CO ratio of the feed kept constant in all the space velocities. Conversion of carbon monoxide and hydrogen, and the formation of various products were measured with a period of 24 h at each space velocity. Periodically during the run, the catalyst activity was measured at preset "standard" condition (a space velocity of 10.4 nl h<sup>-1</sup> g<sub>Fe</sub><sup>-1</sup>) to check the catalyst deactivation. The water partial pressure was determined by collecting the water in the trap, separating it from the oil, and weighing. The weight of water was converted to partial pressure in the reactor based upon the ideal gas law.

The products were analyzed by means of three gas chromatographs, a Shimadzu 4C gas chromatograph equipped with two subsequent connected packed columns: Porapak Q and Molecular Sieve 5A, and a thermal conductivity detector (TCD) with Ar as carrier gas, which was used as a carrier gas for hydrogen analysis. A Varian CP 3800 with a chromosorb column and a thermal conductivity detector (TCD) were used for CO, CO<sub>2</sub>, CH<sub>4</sub>, and other incondensable gases. A Varian CP 3800 with a Petrocol™ DH100 fused silica capillary column and a flame ionization detector (FID) were used for organic liquid products so that a complete product distribution could be provided.

## 3. Results and discussion

### 3.1. Kinetic models

Two mechanisms have been proposed for the WGS reaction over metal oxide catalysts in a non-FT environment: formate and direct oxidation mechanisms (Van der Laan and Beenackers, 1999, 2000; Teng et al., 2005). The direct oxidation mechanism comprises oxidation–reduction cycles. In this mechanism it is assumed that water adsorbs and dissociates on reduced sites to produce hydrogen while oxidizing the site. In the following step, CO is oxidized to CO<sub>2</sub> and reduces the oxidized site to complete the cycle. In another mechanism, it is assumed that adsorbed intermediate (possibly a formate species) is formed through reaction between carbon monoxide and a hydroxyl species or water, which then decomposes to H<sub>2</sub> and CO<sub>2</sub>. The hydroxyl intermediate is formed via decomposition of water.

On the basis of the formate intermediate (WGS I, WGS II) and direct oxidation mechanism (WGS III) for the WGS reaction, three sets of elementary reactions for the WGS reaction are derived in this work, and are listed in Table 1. For the derivation of the rate expressions, the WGS reaction and the FTS reaction (hydrocarbon formation) were assumed to proceed on different active sites, and one rate-determining step was assumed in the sequence of WGS elementary reactions. The remaining steps can be considered to be at quasi-equilibrium and other steps are regarded as fast reversible processes, for which the equilibrium assumption can be used. On basis of the mentioned assumptions, three kinetic rate equations were developed and the expressions are given in Table 2. In these rate equations,  $P_j$  is the partial pressure of species  $j$  in the effluent stream and  $K_p$  is the equilibrium constant of the WGS reaction. For the temperature dependency of the equilibrium constant of the WGS reaction,  $K_p$ , the following relation was used (Van der Laan and Beenackers, 2000):

$$\log K_p = \left( \frac{P_{\text{CO}_2} P_{\text{H}_2}}{P_{\text{CO}} P_{\text{H}_2\text{O}}} \right)_{\text{eq},T} = \left( \frac{2073}{T} - 2.029 \right) \quad (3)$$

where  $K_p$  is the WGS equilibrium constant at the temperature  $T$ . The reaction rate of CO<sub>2</sub> formation was calculated from a material balance over the reactor, assuming ideal gas behavior. Normalizing

**Table 1**  
Elementary reaction steps for WGS reaction.

Model	Reaction step	Elementary reaction
WGS I	1	$\text{CO} + \text{s} \leftrightarrow \text{COs}$
	2	$\text{CO}_2 + \text{s} \leftrightarrow \text{CO}_2\text{s}$
	3	$\text{H}_2\text{O} + \text{s} \leftrightarrow \text{H}_2\text{Os}$
	4	$\text{H}_2 + 2\text{s} \leftrightarrow 2\text{Hs}$
	5 rate-determining step	$\text{COs} + \text{H}_2\text{Os} \leftrightarrow \text{HCOOs} + \text{Hs}$
	6	$\text{HCOOs} + \text{s} \leftrightarrow \text{Hs} + \text{CO}_2\text{s}$
WGS II	1	$\text{CO} + \text{s} \leftrightarrow \text{COs}$
	2	$\text{CO}_2 + \text{s} \leftrightarrow \text{CO}_2\text{s}$
	3	$\text{H}_2\text{O} + \text{s} \leftrightarrow \text{H}_2\text{Os}$
	4	$\text{H}_2\text{Os} + \text{s} \leftrightarrow \text{OHs} + \text{Hs}$
	5	$\text{H}_2 + 2\text{s} \leftrightarrow 2\text{Hs}$
	6 rate-determining step	$\text{COs} + \text{OHs} \leftrightarrow \text{HCOOs} + \text{s}$
	7	$\text{HCOOs} + \text{s} \leftrightarrow \text{Hs} + \text{CO}_2\text{s}$
WGS III	1	$\text{CO} + \text{s} \leftrightarrow \text{COs}$
	2	$\text{H}_2 + 2\text{s} \leftrightarrow 2\text{Hs}$
	3	$\text{H}_2\text{O} + 2\text{s} \leftrightarrow \text{OHs} + \text{Hs}$
	4	$\text{OHs} + \text{s} \leftrightarrow \text{Os} + \text{Hs}$
	5	$\text{COs} + \text{Os} \leftrightarrow \text{CO}_2\text{s} + \text{s}$
	6 rate-determining step	$\text{CO}_2\text{s} \leftrightarrow \text{CO}_2 + \text{s}$

the concentrations of all the intermediates on the catalyst surface leads to:

$$[\text{s}] + [\text{Hs}] + [\text{COs}] + [\text{H}_2\text{Os}] + [\text{OHs}] + [\text{COOs}] = 1 \quad (4)$$

But some simplifications in driving the rate expression equation (Table 2) can be considered based on previous knowledge about adsorbed species on the magnetic sites. In the first kinetic expression WGS I, it is assumed that the adsorption of  $\text{H}_2$ ,  $\text{OH}$  and  $\text{CO}_2$  relative to  $\text{CO}$  and  $\text{H}_2\text{O}$  are negligible and formation of formate intermediate is rate-determining step. In the second model (WGS II) it is assumed that  $\text{H}_2\text{O}$  was being dissociatively adsorbed, and by considering the formation of formate intermediate (reaction step 6) as the rate-determining step and assuming that adsorption of  $\text{H}_2$ ,  $\text{H}_2\text{O}$  and  $\text{CO}_2$  are negligible relative to  $\text{CO}$  and  $\text{OH}$ , the kinetics expression WGS II was obtained.

Model WGS III is based on oxidation–reduction mechanism. In this series of reactions, dissociation of hydroxyl  $\text{CO}_2$  desorption reaction (reaction step 6) can be regarded as rate determination step, based on thermodynamic considerations. If  $\text{CO}_2$  desorption reaction is rate-determining step, in that case the concentration of the adsorbed species  $[\text{CO}_2\text{s}]$  can be considered to be much larger than those of the other adsorbed species and, therefore, the kinetic expression WGS III was obtained.

The model parameters were calculated from the experimental data by minimizing the  $\chi^2$  function with the Levenberg–Marquardt (LM) algorithm, with all experimental reaction rates (Press et al., 1989):

$$\chi^2 = \sum \frac{(R_{\text{exp}} - R_{\text{mod}})^2}{\delta^2} \quad (5)$$

where  $\delta^2$  is the relative variance of the experimental selectivities in the WGS reaction rate. In this approach, the difference between the

measured and predicted rates is divided by the standard deviation of the involved rate measurement. Data points with a high accuracy have low standard deviations and therefore count more heavily towards the sum of errors than inaccurate data. In other words, the weight (importance) assigned to each observation is related to the accuracy of that specific measurement. The variance is due to experimental inaccuracies and *lack of fit* of the kinetic model. Confidence limits on the estimated model parameters were calculated at a 95% confidence level. Whereas the value of chi-square was used for model optimization and discrimination, the mean absolute relative residual (MARR) is reported as a measure of the goodness of fit:

$$\text{MARR} = 100 \sum_{i=1}^n \left| \frac{R_{\text{exp}} - R_{\text{mod}}}{R_{\text{exp}}} \right| \frac{1}{n} \quad (6)$$

where  $n$  is the number of data points included. The estimates of the kinetic parameters must have physical relevance. Rate models yielding negative adsorption coefficients were excluded for further model discrimination. Furthermore, the surface fractions of adsorbed species should be realistic and the residuals between model and experiment should be normally distributed with zero average and may not observe trends as a function of the independent variables. The discrimination between the rival models and the estimation of the parameter values was performed using the experiments at 563 K.

### 3.2. Catalytic performance

An estimation of the extent of the water-gas shift reaction can be obtained by the following the WGS reaction quotient ( $\text{RQ}_{\text{WGS}}$ ) (Raje et al., 1998):

$$\text{RQ}_{\text{WGS}} = \frac{P_{\text{CO}_2} P_{\text{H}_2}}{P_{\text{CO}} P_{\text{H}_2\text{O}}} \quad (7)$$

where  $P_j$  is the partial pressure of species  $j$  in the effluent stream. The approach to the WGS equilibrium can be described by the parameter  $\eta$ , obtained by dividing the WGS reaction quotient by the equilibrium constant at the reaction temperature (Botes, 2007; Krishnammorrthy et al., 2002):

$$\eta = \frac{1}{K_p} \left( \frac{P_{\text{CO}_2} P_{\text{H}_2}}{P_{\text{CO}} P_{\text{H}_2\text{O}}} \right) \quad (8)$$

The value of  $\eta$  ranged from 0 to 1, the latter being the equilibrium value (Krishnammorrthy et al., 2002). It is shown in Fig. 1 that the experimental values over the wide reaction conditions in this kinetic study are much less than the equilibrium values  $K_p$ . In general, the value of  $\eta$  (and subsequently of the reaction quotient) was small at low carbon monoxide conversions and increased at higher carbon monoxide conversions and also it is, in good agreement with previous studies (Teng et al., 2005; Botes, 2007; Krishnammorrthy et al., 2002). This indicates that the WGS reaction under FTS reaction conditions is far from equilibrium, which is also observed by others (Teng et al., 2005; Botes, 2007; Krishnammorrthy et al., 2002). The value of  $\eta$  versus the reaction

**Table 2**  
Rate expressions considered for the WGS reaction,  $R_{\text{CO}_2}$  ( $\text{mmol g}_{\text{cat}}^{-1} \text{s}^{-1}$ )

Model	Kinetic equation	Site balance
WGS I	$R_{\text{CO}_2} = k_w (P_{\text{CO}} P_{\text{H}_2\text{O}} - P_{\text{CO}_2} P_{\text{H}_2} / K_p) / (1 + K_1 P_{\text{CO}} + K_3 P_{\text{H}_2\text{O}})^2$ $k_w = k_5 K_1 K_3 \text{ (mmol g}_{\text{cat}}^{-1} \text{s}^{-1} \text{ bar}^{-2})$	$\text{s} + \text{COs} + \text{H}_2\text{Os}$
WGS II	$R_{\text{CO}_2} = k_w (P_{\text{CO}} P_{\text{H}_2\text{O}} / P_{\text{H}_2}^2 - P_{\text{CO}_2} P_{\text{H}_2}^2 / K_p) / (1 + K_1 P_{\text{CO}} + K P_{\text{H}_2\text{O}} / P_{\text{H}_2}^2)^2$ $k_w = k_5 K_1 K_3 K_4 K_5^{-1/2} \text{ (mmol g}_{\text{cat}}^{-1} \text{s}^{-1} \text{ bar}^{-3/2})$ $K = K_4 K_3 / K_5^2$	$\text{s} + \text{COs} + \text{OHs}$
WGS III	$R_{\text{CO}_2} = k_w (P_{\text{CO}} P_{\text{H}_2\text{O}} / P_{\text{H}_2} - P_{\text{CO}_2} / K_p) / (1 + K P_{\text{CO}} P_{\text{H}_2\text{O}} / P_{\text{H}_2})$ $k_w = k_6 K_1 K_2^{-1/2} K_3 K_4 K_5 \text{ (mmol g}_{\text{cat}}^{-1} \text{s}^{-1} \text{ bar}^{-1})$	$\text{s} + \text{CO}_2\text{s}$

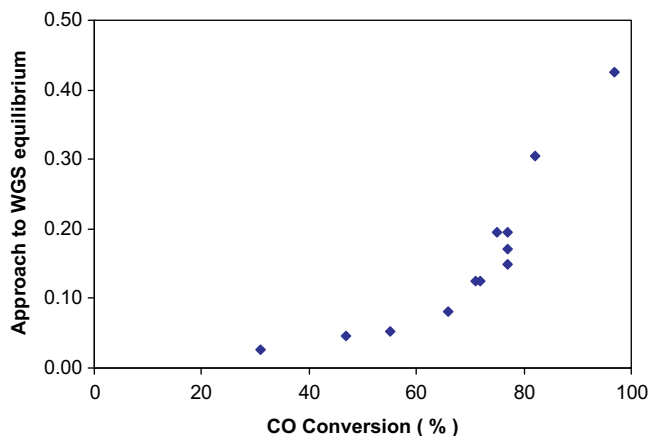


Fig. 1. Approach to the WGS equilibrium vs. CO conversion (%).

temperature is represented in Fig. 2. Carbon monoxide conversion improved as the reaction temperature increased, and as shown in Fig. 2, the approach to the WGS equilibrium ( $\eta$ ) was increased.

### 3.3. Isothermal discrimination

In order to check systematic isothermal discrimination, the agreement between each of the rival rate equations and the measured reaction rates was presented as a function of the approach to WGS equilibrium. Fig. 3 shows that the errors in prediction of WGS regarding the models with the approach to equilibrium, these plots show a systematic deviation in the models based on oxidation–reduction cycles which may be indicative of a fundamental incorrectness in the expressions. In contrast, the deviations in the models based on the formate mechanism appear to be random scatter rather than consistent errors. As shown in this figure, at higher approach to WGS equilibrium ( $\eta$ ), deviation from one in all models was increased. It is known that the WGS reaction and FTS reaction occur on the different types of sites and the two reactions will only influence each other via the gas phase of reactants. Meanwhile, the FTS reaction depends highly on the hydrogen formed by the WGS reaction. Thus, the overall FTS rate affected by the rate/extent of the WGS reaction at high conversions. The deviation from one in all models may be related to this conjugation of FTS and WGS reactions (Raje et al., 1998).

The WGS reaction rate was optimized with the kinetic expressions in Table 2. The corresponding model parameters and related MARR value and weighted sum of errors ( $\chi^2$ -value) are also given in Table 3. In this table, the parameters of  $K_1$ ,  $K_3$ , and  $K$  for WGS I, WGS

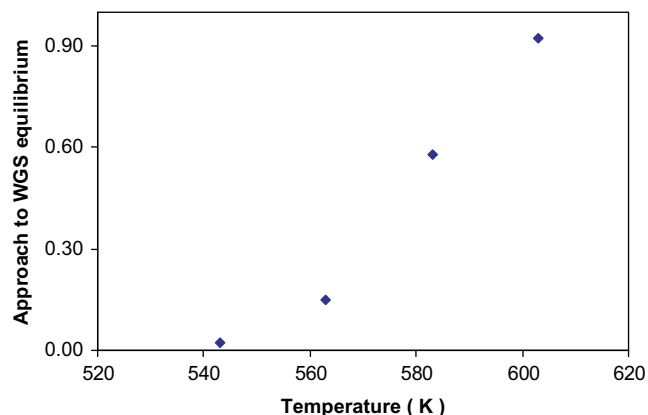


Fig. 2. Approach to the WGS equilibrium vs. reaction temperature.

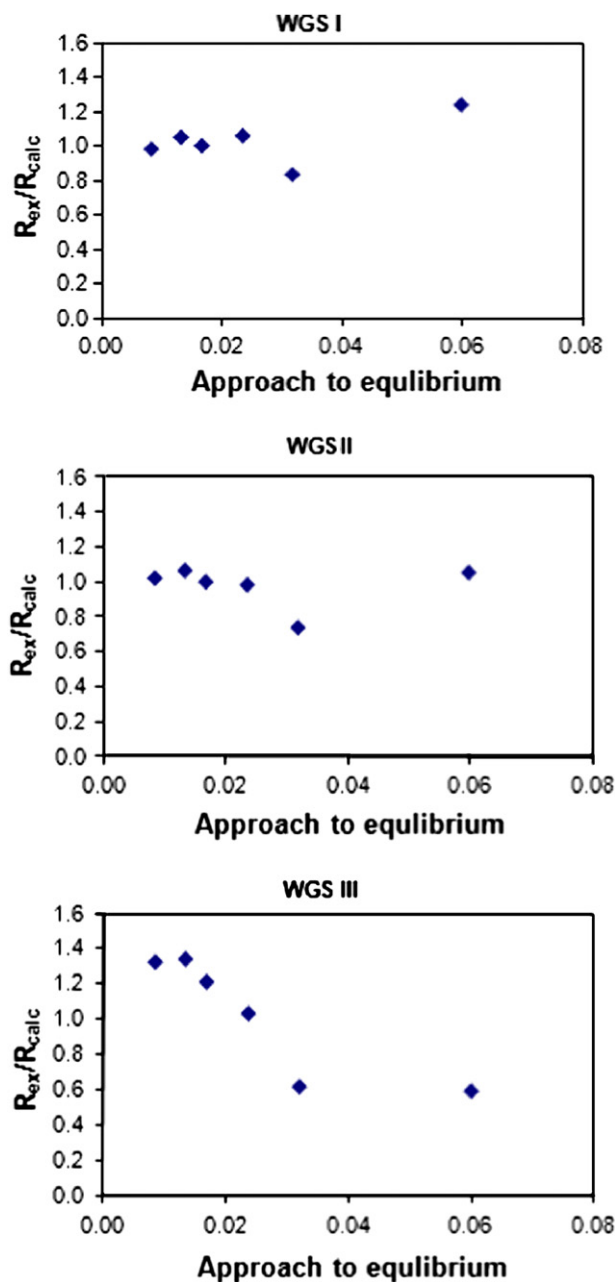


Fig. 3. Comparison of the calculated and experimental  $\text{CO}_2$  flow rates as the WGS reaction approaches equilibrium.

II are related to adsorption coefficients of CO,  $\text{H}_2\text{O}$ , and hydroxyl groups expressions, respectively. However, the parameter  $K$  in WGS III expression is related to adsorption coefficients of adsorbed  $\text{CO}_2$  in rate-determining step. It should further be noted that the adsorption coefficients of CO or CO containing intermediates are small compared to the adsorption coefficients of water or hydroxyl groups. This is in agreement with the results of other studies on the WGS reaction in the iron-based FTS synthesis (Van der Laan and Beenackers, 2000; Botes, 2007). From Table 3, we can find that the WGS kinetic model obtained from the formate mechanism is better than the model obtained from the direct oxidation mechanism for fitting experimental data. A possible explanation is that the dissociation of hydroxyl intermediate to adsorbed oxygen and hydrogen is not energetically favorable under FTS reaction conditions. This is also supported by quantum calculation on transition metals that the hydroxyl dissociation is energetically unfavorable

**Table 3**  
WGS kinetics model parameters.

Model	Kinetic parameters	$\chi^2$	MARR (%)
WGS I	$k_w = 0.77 \text{ mmol g}_{\text{cat}}^{-1} \text{ s}^{-1} \text{ bar}^{-2}$ $K_1 = 0.39 \text{ bar}^{-1}, K_3 = 3.54 \text{ bar}^{-1}$	870	8.73
WGS II	$k_w = 1.20 \text{ mmol g}_{\text{cat}}^{-1} \text{ s}^{-1} \text{ bar}^{-3/2}$ $K_1 = 0.60 \text{ bar}^{-1}, K = 5.51 \text{ bar}^{-1}$	984	9.15
WGSIII	$k_w = 0.12 \text{ mmol g}_{\text{cat}}^{-1} \text{ s}^{-1} \text{ bar}^{-1}$ $K = 1.92 \text{ bar}^{-1}$	2750	21.94

with a relatively high activation barrier (Wu et al., 2004; Michaelides and Hu, 2001).

Fig. 4 compares the experimental and calculated WGS reaction rates of assume models. In this figure,  $R^2$  is a parameter for

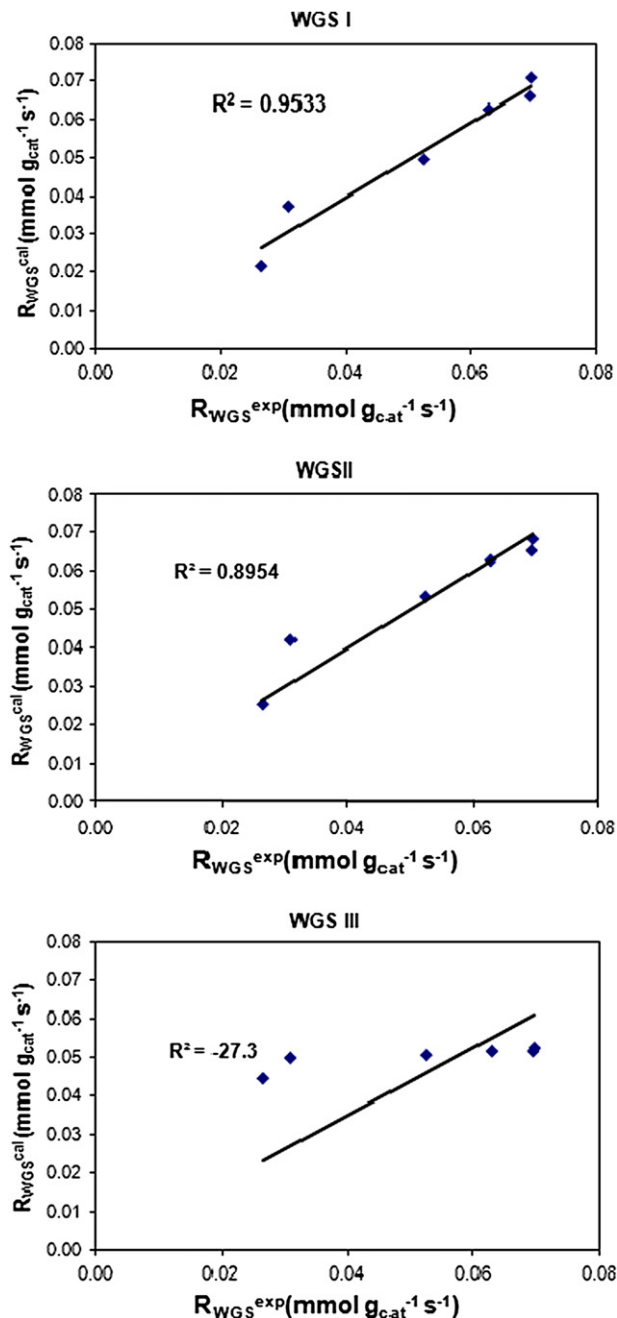


**Fig. 4.** Comparison between calculated and experimental  $\text{CO}_2$  flow rates.  $R^2 = 1 - (\text{Residual sum of squares})/(\text{Corrected sum of squares})$ .

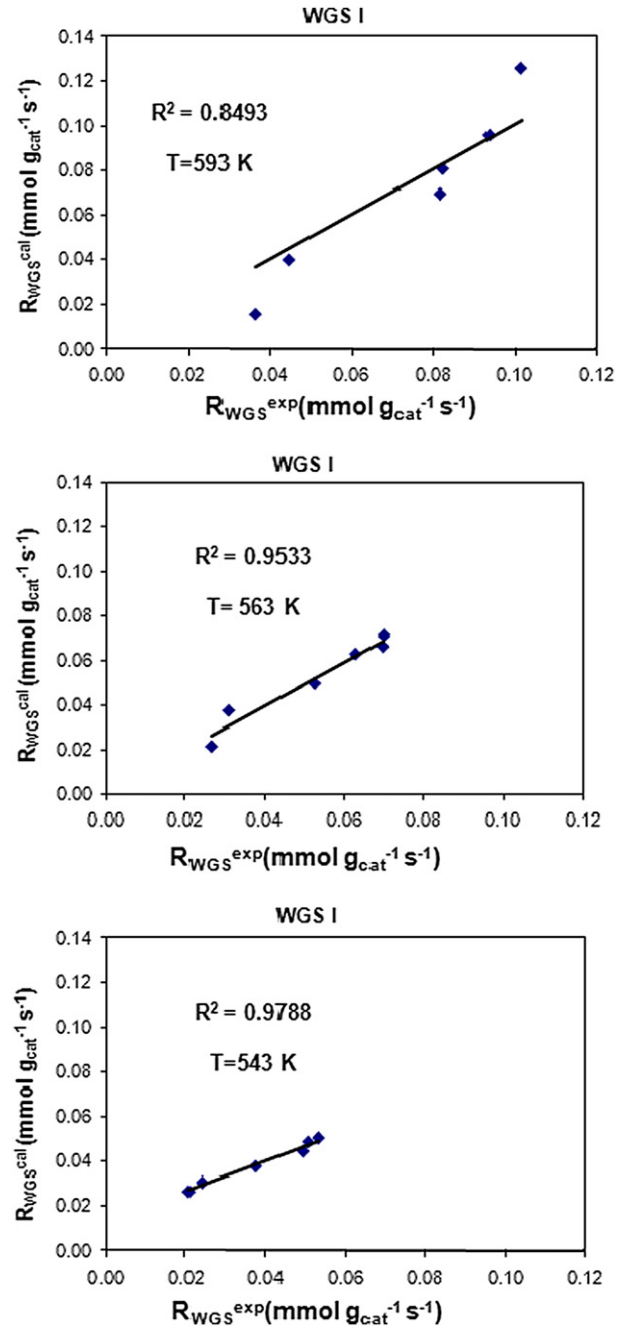


**Fig. 5.** Comparison between calculated and experimental  $\text{CO}_2$  flow rates by WGS I model at various temperatures.  $R^2 = 1 - (\text{Residual sum of squares})/(\text{Corrected sum of squares})$ .

discrimination of results and it is compared calculated and experimental WGS reaction rates and defined as:

$$R^2 = 1 - (\text{Residual sum of squares})/(\text{Corrected sum of squares}) \quad (9)$$

According to the MARR value and weighted sum of errors ( $\chi^2$ -value) in Table 3, and value of  $R^2$  in Fig. 4, it can be concluded that WGS I model is the best kinetic model for fitting from the experimental data between three models introduced in Table 1. From Table 3, it is also found that the elementary reaction of  $\text{H}_2\text{O}$  dissociation is not an important step in the WGS reaction under the FTS conditions. This indicates that the kinetic methods cannot

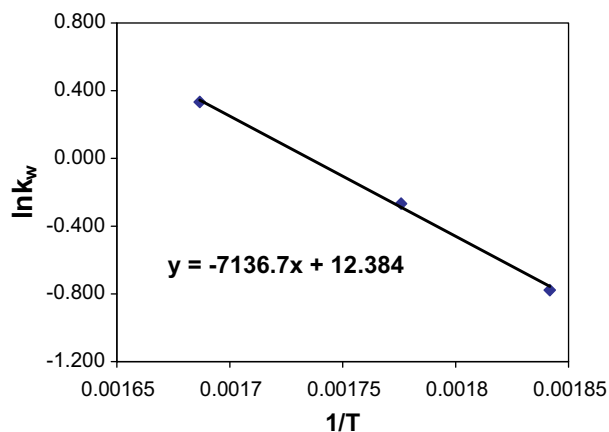


Fig. 6. Plots of the calculated WGS rate constant ( $k_w$ ) ( $\text{mmol g}_{\text{cat}}^{-1} \text{s}^{-1} \text{bar}^{-2}$ ) vs. reciprocal temperature ( $\text{K}^{-1}$ ).

discriminate whether water reacts as associative or dissociative form in the surface reaction. This conclusion is also supported by others (Teng et al., 2005).

Reaction rate expression WGS I is similar to the optimal model of Van der Laan and Beenackers (1999). This model assumes that the rate of the WGS reaction is determined by the reaction of adsorbed carbon monoxide and hydroxyl toward a formate intermediate and adsorption of CO and water to be dominated in the site balance. WGSII model assumed that the rate of the WGS reaction is determined by the reaction of adsorbed carbon monoxide and hydroxyl toward a formate intermediate. In reaction rate expression WGSII, it is assumed that adsorption of CO and hydroxyl species are dominated in the site balance which is present in the rate-determining step. From Table 3, it should also be noted that the adsorption coefficients of CO or CO containing intermediates, are small in comparison with the adsorption coefficients of water or hydroxyl groups, and adsorption coefficients of hydroxyl groups is higher than water.

Botes (2007) reported that WGS sites are mainly covered by water and/or hydroxyl species in the Fe-low temperature FT synthesis. This is different from the findings of this work. The results of the present work shows that by increasing the temperature in FT reaction the concentration of CO adsorbed on the WGS catalytic sites was increased and must be considered in reaction rate expression like as reported by Van der Laan and Beenackers (2000).

### 3.4. Calculation of WGS activation energy

Comparison of calculated and experimental  $\text{CO}_2$  flow rates in WGS I model at various temperatures are presented in Fig. 5. As shown in this figure by increasing the reaction temperature, deviation between predicted and experimental results is increased because at higher temperatures FTS reaction highly depends on the hydrogen formed by the WGS. Thus, the overall FTS reaction rate is highly affected by the rate/extent of the WGS reaction at high FTS conversions. Also as shown in Fig. 2, the value of  $\eta$  (the approach to the WGS equilibrium) at higher temperature was increased and WGS reaction reached to equilibrium condition.

Table 4  
WGS kinetics data, obtained based WGS I model.

Catalyst	$k_w(\text{mmol g}_{\text{cat}}^{-1} \text{s}^{-1} \text{bar}^{-2})$			$E_a$ (kJ)
	543 K	563 K	593 K	
Fe/Cu/La/Si nano struct.	0.46	0.77	1.40	59

The temperature dependence of the reaction rate constants is evaluated according to the Arrhenius-type equation:

$$k_w(T) = A \cdot \exp(-E_a/RT) \quad (10)$$

Hence, a plot of  $\ln(k)$  versus  $1/T$  should give a straight line with slope of  $-E_a/R$ . The logarithm of the rate constant ( $k$ ) is plotted in Fig. 6 as a function of reverse of temperature for catalysts. From the slope of the curves in Fig. 6, the activation energy is determined 59 kJ/mol and listed in Table 4. Also Table 4 lists the WGS kinetic data obtained based WGS I model. These calculated activation energy indicate that although the WGS reaction and FTS reaction occur on the different types of sites, both reactions will influence on each other via the gas phase of reactants and WGS reaction is active in FTS reaction system (Wang et al., 2003; Raje et al., 1998).

## 4. Conclusions

A number of Langmuir–Hinshelwood–Hougen–Watson type rate equations were derived on the basis of formate and direct oxidation mechanisms. For derivation of the rate expressions, several assumptions were made: the WGS reaction and FTS reaction are assumed to proceed on different active sites, one rate-determining step (RDS) in the sequence of elementary WGS reactions and the surface concentration of the intermediates that take part in the rate-determining reaction is much higher than that of the other intermediates. WGS rate expressions based on the formate mechanism were found to provide an improved description of the WGS kinetic data.

These results indicate that the kinetic methods cannot discriminate whether water reacts as associative or dissociative form in the surface reaction and by increasing the temperatures in FTS reaction the concentration of CO adsorbed on the WGS catalytic sites was increased and must be considered in reaction rate expression. These calculated activation energy indicate that although the WGS reaction and FTS reaction occur on the different types of sites, but these reactions will influence each other via the gas phase of reactants and WGS reaction is active in FTS reaction system. Kinetic experimental results show that the WGS reaction under FTS reaction conditions is far from equilibrium.

## References

- Anderson, R.B., 1984. The Fischer–Tropsch Synthesis. Academic Press, Orlando, FL.
- Bartholomew, C.H., 1991. Recent Developments in Fischer–Tropsch Catalysis, New Trends in CO Activation, Studies in Surface Science and Catalysis, No. 64. Elsevier, Amsterdam.
- Botes, F.G., 2007. Appl. Catal. A: Gen. 328, 237.
- Dry, M.E., 1981. In: Anderson, J.R., Bourdard, M. (Eds.), Catalysis Sciences and Technology, vol. 1. Springer-Verlag Chapter 4.
- Eriksson, S., Nylén, U., Rojas, S., Boutonnet, M., 2004. Appl. Catal. A: Gen. 265, 207.
- Guo, X., Liu, Y., Chang, J., Bai, L., Xu, Y.Y., Xiang, H.W., Li, Y.W., 2006. J. Nat. Gas Chem. 15, 105.
- Herranz, T., Rojas, S., Pérez-Alonso, F.J., Ojeda, M., Terreros, P., Fierro, J.L.G., 2006. Appl. Catal. A: Gen. 311, 66.
- Jin, Y.M., Datye, A.K., 2000. J. Catal. 196, 8.
- Jothimurugesan, K., Goodwin, J.G., Santosh, S.K., Spivey, J.J., 2000. Catal. Today 58, 335.
- Krishnamoorthy, S., Li, A., Iglesia, E., 2002. Catal. Lett. 80, 77.
- Michaelides, A., Hu, P., 2001. J. Am. Chem. Soc. 123, 4235.
- Nakhaei Pour, A., Shahri, S.M.K., Zamani, Y., Irani, M., Tehrani, S., 2008a. J. Nat. Gas Chem. 17, 242.
- Nakhaei Pour, A., Zamani, Y., Tavasoli, A., Shahri, S.M.K., Taheri, S.A., 2008b. Fuel 87, 2004.
- Nakhaei Pour, A., Shahri, S.M.K., Bozorgzadeh, H.R., Zamani, Y., Tavasoli, A., Marvast, M.A., 2008c. Appl. Catal. A: Gen. 348, 201.
- Nakhaei Pour, A., Taghipoor, S., Shekarriz, M., Shahri, S.M.K., Zamani, Y., 2009a. J. Nanosci. Nanotechnol. 9, 4425.
- Nakhaei Pour, A., Zare, M., Shahri, S.M.K., Zamani, Y., Alaei, M.R., 2009b. J. Nat. Gas Sci. Eng. 1, 183.
- Nakhaei Pour, A., Housaindokht, M.R., Tayyari, S.F., Zarkesh, J., 2010a. J. Nat. Gas Chem. 19, 107.

- Nakhaei Pour, A., Housaindokht, M.R., Tayyari, S.F., Zarkesh, J., Alaei, M.R., 2010b. *J. Nat. Gas Sci. Eng.* 2 (2–3), 61–68.
- Press, W.H., Flannery, B.P., Teukolsky, S.A., Vetterling, W.T., 1989. *Numerical Recipes in Pascal*. Cambridge University Press, New York.
- Raje, A.P., Brien, R.J.O., Davis, B.H., 1998. *J. Catal.* 180, 36.
- Sarkar, A., Seth, D., Dozier, A.K., Neathery, J.K., Hamdeh, H.H., Davis, B.H., 2007. *Catal. Lett.* 117, 1.
- Schwuger, M.J., Stickdorn, K., Schomacker, R., 1995. *Chem. Rev.* 95, 849.
- Teng, B.T., Cheng, J., Yang, J., Wang, G., Zhang, C.H., Xu, Y.Y., Xiang, H.W., Li, Y.W., 2005. *Fuel* 84, 917.
- Van der Laan, G.P., Beenackers, A.A.C.M., 1999. *Catal. Rev. Sci Eng.* 41, 255.
- Van der Laan, G.P., Beenackers, A.A.C.M., 2000. *Appl. Catal. A: Gen.* 193, 39.
- Wang, Y.N., Ma, W.P., Lu, Y.J., Yang, J., Xu, Y.Y., Xiang, H.W., Li, Y.W., Zhao, Y.L., Zhang, B.J., 2003. *Fuel* 82, 195.
- Wu, B.S., Bai, L., Xiang, H.W., Li, Y.W., Zhang, Z.X., Zhong, B., 2004. *Fuel* 83, 205.